**INTERNATIONAL JOURNAL OF OPTIMIZATION IN CIVIL ENGINEERING**
***Int. J. Optim. Civil Eng., 2017; 7(1):109-127***

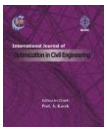

# OPTIMIZATION FORMULATION FOR NONLINEAR STRUCTURAL ANALYSIS

M. Rezaiee-Pajand[*, †] and H. Afsharimoghadam
*Civil Engineering Department, Ferdowsi University of Mashhad*

## ABSTRACT

In this paper, the effect of angle between predictor and corrector surfaces on the structural analysis is investigated. Two objective functions are formulated based on this angle and also the load factor. Optimizing these functions, and using the structural equilibrium path's geometry, lead to two new constraints for the nonlinear solver. Besides, one more formula is achieved, which was previously found by other researchers, via a different mathematical process. Several benchmark structures, which have geometric nonlinear behavior, are analyzed with the proposed methods. The finite element method is utilized to analyze these problems. The abilities of suggested schemes are evaluated in tracing the complex equilibrium paths. Moreover, comparison study for the required number of increments and iterations is performed. Results reflect the robustness of the authors' formulations.

**Keywords:** optimization; path-following analysis; geometric nonlinear behavior; constraint equality; load-displacement curve; limit points.

Received: 2 April 2016; Accepted: 12 June 2016

## 1. INTRODUCTION

Nonlinear analysis expresses the real behavior of structures under different types of loading. In other words, to find actual structural performances, material or geometric nonlinear behavior should be investigated. So far, a lot of different strategies for nonlinear structural analysis have been suggested. These techniques have their own merits and demerits, and yet; no perfect procedure is available. As notified in the literature review, an accurate method to trace the whole equilibrium paths of all structures has not been proposed until now.

[*]Corresponding author: Civil Engineering Department, Ferdowsi University of Mashhad
[†]E-mail address: rezaiee@um.ac.ir (M. Rezaiee-Pajand)

Newton-Raphson algorithm is one of the most popular foundations of iterative methods [1]. Due to the failure of Newton-Raphson techniques on crossing snap-through regions, the displacement control procedure was introduced [2]. This solution was not able to passing through snap-back regions. In the 70's, Wempner [3] and Riks [4] invented arc length methods. They defined the arc length parameter as the distance of the last static point to the supposed iteration path. The approach of finding arc length parameter led first to the normal plane method [5] and then, to the updated normal plane technique [6].

In the constraint equation of the cylindrical arc length method, Crisfield ignored the force component [7]. He named his proposed solver, modified Riks-Wempner procedure. Subsequently, Tsai *et al.* used arc length algorithm in finite element method for analyzing of a composite cylindrical shell-like structure [8]. Some researchers minimized effective variables of the nonlinear analysis. Reduced residual load by Bergan [9], residual displacement by Chan [10] and residual length, perimeter and area in the research of Rezaiee-Pajand *et al.* [11], were minimized. In 1990, Yang *et al.* introduced generalized displacement control (GDC) method that could catch both load, and displacement limit points [12]. Cardoso *et al.* detected this efficient strategy, GDC method, as an orthogonal cylindrical arc length method [13]. In normal flow scheme, sequential iterative analyses on lines, which were perpendicular to Davidenko's flow, were implemented to reach the structural equilibrium path [14]. Afterward, Saffari *et al.* formulated improved normal flow scheme [15].

On the other hand, the dynamic relaxation (DR) method was performed for post-buckling analysis of trusses [16]. Rezaiee-Pajand *et al.* applied DR technique in the nonlinear analysis for various structures [17, 18]. This capable algorithm set up a fictitious dynamic system to solve the nonlinear system of equations governing the structural behavior. Recently, Rezaiee-Pajand *et al.* created an efficient strategy by combining DR method with load factor and displacement increments [19]. From a strictly mathematical viewpoint, it could be implied to multi-point procedures with different convergence [20, 21]. In an extensive research, the geometric nonlinear analysis methods of structures were investigated and compared with each other [22].

Geometric nonlinear behavior is due to the structural large deformations. To perform this analysis, researchers found diverse constraint relations with different assumptions. According to the related literature, no accurate method to trace the whole equilibrium paths of all structures has not been proposed until now. In the present study, the geometries of predictor and corrector steps' path are surveyed, and two objective functions are formed. Each of them has two independent variables. By this mathematical base, two novel constraint equations are created. Furthermore, one more constraint formula is concluded, which was found by other investigators in a different way. This outcome clearly demonstrates the validity of assumptions and formulations' process. It has been shown that the geometric nonlinear behavior can lead to various complex structural static paths. To explore these performances, and show the abilities of the authors' techniques, several two and three-dimensional trusses and planar frames are nonlinearly analyzed by exerting proposed constraints.

## 2. SOLVING NONLINEAR EQUATIONS

Governing equation of the nonlinear behavior of structures is as follows:

$$R(u,\lambda) = \lambda P - F(u) \tag{1}$$

In the current equality, displacement vector, load factor, residual load vector, external force vector and internal force vector are shown by $u$, $\lambda$, $R(u,\lambda)$, $P$ and $F(u)$, respectively. Residual load vector depends on the displacement and load factor variables. It has been emphasized that the load factor has an important role in the nonlinear structural analysis. If the displacement vector has m arrays, then the system of Equations (1) will have m+1 unknowns. The extra unknown for a structure with m degrees of freedom is because of $\lambda$. Hence, for calculating the unknowns, one more relation is required in addition to Equations (1). Based on Fig. 1, in the n-th incremental step, the process of analysis is accomplished to find the structural equilibrium curve between n-1-th and n-th points. In the predictor step, to discover displacement increment in Equation (2), a suitable incremental load should be supposed.

$$\Delta u_1^n = (K^{n-1})^{-1} \times \Delta\lambda_1^n P \tag{2}$$

In this relation, $K^{n-1}$ is the tangential stiffness matrix at the n-1-th point of the structural static curve. In the n-th incremental step, the coordinates of the first iteration point is accessed by Equality (2). Consecutive iterations are done to get beyond the point n within a defined tolerance. The load factor of each iteration is computed by constraint relation. It should be mentioned, displacement increment of the successive iteration steps is calculated by following linear equality [23]:

$$\delta u_i^n = \delta u_i''^n + \delta\lambda_i^n \delta u_i'^n \tag{3}$$

Superscript $n$ and subscript $i$ represent the increment and iteration number of analysis, respectively. In the recent equation, $\delta u_i''^n$ and $\delta u_i'^n$ are the displacement increments due to residual load and external force, correspondingly. These vectors are defined in the following relations:

$$\delta u_i''^n = (K_i^n)^{-1} \times R_i^n \tag{4}$$

$$\delta u_i'^n = (K_i^n)^{-1} \times P \tag{5}$$

In fact, the values of forces $R$ and $P$ are known at the beginning of each iteration. Therefore, their related displacements are available. According to Equation (3), finding $\delta u_i^n$

only depends on the load factor. Based on the succeeding relations, the load factor and displacement increments of structure are gained by adding $\delta\lambda_i^n$ and $\delta u_i^n$ to their previous increments, correspondingly:

$$\Delta\lambda_{i+1}^n = \Delta\lambda_i^n + \delta\lambda_i^n \tag{6}$$

$$\Delta u_{i+1}^n = \Delta u_i^n + \delta u_i^n \tag{7}$$

It is worth mentioning that in the former proposed methods, the positions of the predictor's path and the corrector's path were assumed arbitrary and then constraint equality was obtained [5-7]. On the contrary, in this study optimal angle between the predictor's path and the corrector's path is achieved by using mathematical tools along with the geometry of the equilibrium curve. Based on the optimized criteria, the relations required for the structural analysis are formulated.

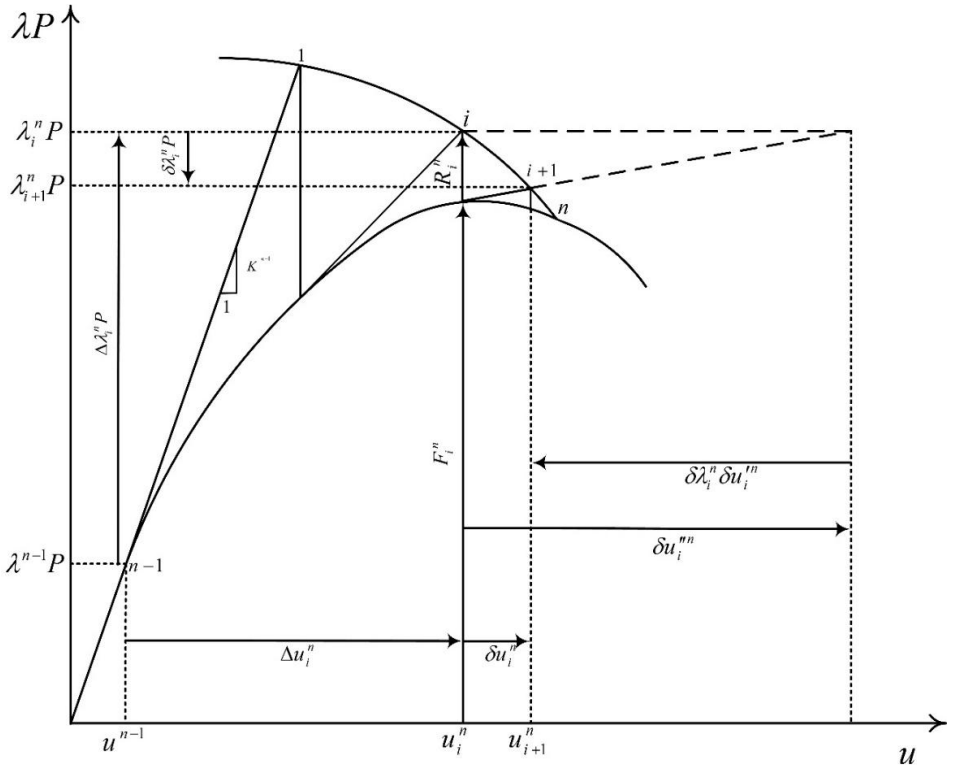


Figure 1. The process of advanced incremental-iterative methods

*2.1 First new method*

In this procedure, the angle, between the tangent of the static points on the structural equilibrium path and the trajectory which passes through the sequential iterative analyses, is

assumed as $\gamma$. Outline of the proposed scheme for the j-th degree of freedom of structure is shown in Fig. 2. Based on this figure, the next relations between the specified angles are available:

$$\alpha+\beta+\gamma=180^\circ \Rightarrow \tan(\beta)=\tan(\pi-(\alpha+\gamma))=-\tan(\alpha+\gamma) \tag{8}$$

where, $\alpha$ and $\beta$ are the angles between the tangent of the static points and its relevant iterative analyses' path with the displacement axis, correspondingly. In accordance with this definition, the tangent of these angles can be determined in the below forms:

$$\tan(\beta)=\frac{\delta\lambda_i^n P}{\delta u_i^n} \tag{9}$$

$$\tan(\alpha)=K_i^n \tag{10}$$

Utilizing the trigonometry commands for Equation (8) and substituting Equation (9) and (10) in it, the succeeding equality is found:

$$\frac{\delta\lambda_i^n P}{\delta u_i^n}=\frac{K_i^n+\tan(\gamma)}{K_i^n\times\tan(\gamma)-1} \tag{11}$$

Inserting Equations (3) and (5) into (11) and simplifying it, conclude the following relationship:

$$\begin{aligned}&\tan(\gamma)\times\delta\lambda_i^n P^T P-2\delta\lambda_i^n P^T\delta u_i'^n-P^T\delta u_i''^n-\tan(\gamma)\times\delta u_i''^{nT}\delta u_i'^n\\&-\tan(\gamma)\times\delta\lambda_i^n\delta u_i'^{nT}\delta u_i'^n=0\end{aligned} \tag{12}$$

It is possible to define the left hand of the current equation as a goal function. Consequently, the next function, $G$, in terms of two independent variables is established:

$$\begin{aligned}&G(\delta\lambda_i^n,\gamma)=\tan(\gamma)\times\delta\lambda_i^n P^T P-2\delta\lambda_i^n P^T\delta u_i'^n-P^T\delta u_i''^n-\tan(\gamma)\times\delta u_i''^{nT}\delta u_i'^n\\&-\tan(\gamma)\times\delta\lambda_i^n\delta u_i'^{nT}\delta u_i'^n\end{aligned} \tag{13}$$

Then, the process of optimizing Function (13), with respect to the angle $\gamma$ and the load factor, has the coming shapes:

$$\frac{\partial G}{\partial\delta\lambda_i^n}=tan(\gamma)\times P^T P-2P^T\delta u_i'^n-tan(\gamma)\times\delta u_i'^{nT}\delta u_i'^n=0 \tag{14}$$

$$\frac{\partial G}{\partial \gamma} = (1+\tan^2(\gamma)) \times (\delta\lambda_i^n P^T P - \delta u_i''^{nT} \delta u_i'^n - \delta\lambda_i^n \delta u_i'^{nT} \delta u_i'^n) = 0 \tag{15}$$

The constraint equality of the first suggested method is obtained by solving the system of two Equations (14) and (15). As a result, the following load factor is calculated:

$$\delta\lambda_i^n = \frac{\delta u_i''^{nT} \delta u_i'^n}{P^T P - \delta u_i'^{nT} \delta u_i'^n} \tag{16}$$

This constraint is used for the geometric nonlinear analysis of the benchmark structures in the next section. If the load component of Equality (16) is neglected, the familiar relation is attained, as follows:

$$\delta\lambda_i^n = -\frac{\delta u_i''^{nT} \delta u_i'^n}{\delta u_i'^{nT} \delta u_i'^n} \tag{17}$$

The last mentioned approximation leads to the outcome of the well-known procedure, called the minimum residual displacement method [10]. In other words, the authors' formulation provides alternative proof of the former scheme, and it shows the generality and rightness of the suggested technique.

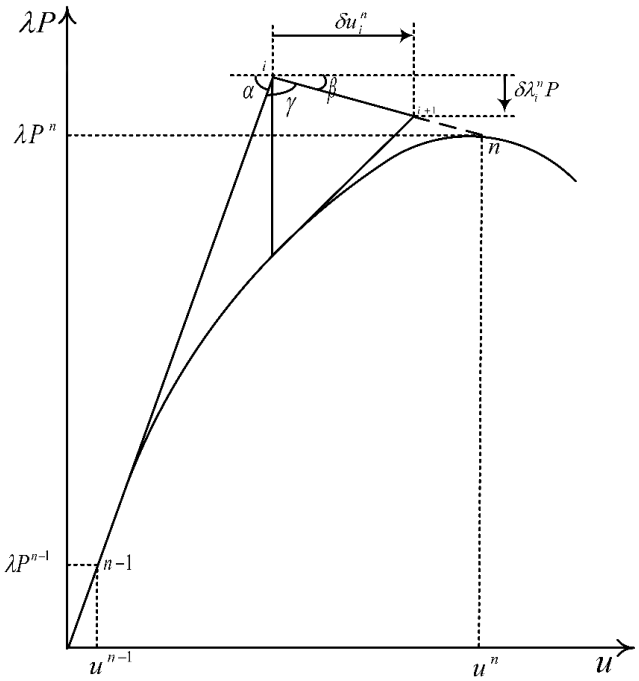


Figure 2: First proposed scheme

*2.2 Second new method*

In this way, the tangential stiffness matrix in the n-1-th point of the equilibrium path ($K^{n-1}$) is utilized. From the geometric viewpoint, this stiffness matrix is denoted in Fig. 1. In fact, it is assumed that the stiffness matrix of iterative steps ($K_i^n$) is equal to $K^{n-1}$. By replacing Equation (3) into Equation (11), the equality is rewritten in the succeeding form:

$$\tan(\gamma)\times K^{n-1}\times\delta\lambda_i^n P-\delta\lambda_i^n P-K^{n-1}\times\delta u_i''^n-K^{n-1}\times\delta\lambda_i^n\delta u_i'^n-\tan(\gamma)\times\delta u_i''^n \\ -\tan(\gamma)\times\delta\lambda_i^n\delta u_i'^n=0 \tag{18}$$

According to the current relation, the next two-variable goal function, $H$ , is proposed:

$$H(\delta\lambda_i^n,\gamma)=\tan(\gamma)\times K^{n-1}\times\delta\lambda_i^n P-\delta\lambda_i^n P-K^{n-1}\times\delta u_i''^n-K^{n-1}\times\delta\lambda_i^n\delta u_i'^n-\tan(\gamma)\times\delta u_i''^n \\ -\tan(\gamma)\times\delta\lambda_i^n\delta u_i'^n \tag{19}$$

To optimize this function, its differentiation with respect to the independent variables should be taken, as follows:

$$\frac{\partial H}{\partial\delta\lambda_i^n}=tan(\gamma)\times K^{n-1}\times P-P-K^{n-1}\times\delta u_i'^n-tan(\gamma)\times\delta u_i'^n=0 \tag{20}$$

$$\frac{\partial H}{\partial\gamma}=(1+\tan^2(\gamma))\times(K^{n-1}\times\delta\lambda_i^n P-\delta u_i''^n-\delta\lambda_i^n\delta u_i'^n)=0 \tag{21}$$

Solving the last system of equations results in the following load factor:

$$\delta\lambda_i^n=\frac{\delta u_i''^n}{K^{n-1}\times P-\delta u_i'^n} \tag{22}$$

By substituting Equation (5) in the recent equality, the last relation can be rewritten in the below form:

$$\delta\lambda_i^n=\frac{K^{n-1}\times\delta u_i''^n}{K^{n-1}\times K^{n-1}\times P-P} \tag{23}$$

The subsequent vector form of the second proposed constraint is achieved by inserting Equation (2) into the current relation:

$$\delta\lambda_i^n=\frac{\Delta\lambda_1^n P^T\delta u_i''^n}{(K^{n-1T}K^{n-1}-1)\times P^T\Delta u_1^n} \tag{24}$$

To perform the analysis process, stiffness matrix must be turned into vector form. To achieve this goal, only main diagonal arrays of the stiffness matrix are utilized. By this action, the stiffness matrix changes into a vector with m components. In this paper, Constraint (24) is also used for the analysis of benchmark structures. To summarize the outcomes, the novel constraints are written in Table 1.

Table 1: Proposed constraints

| Method | Constraint |
|---|---|
| First method | $\delta\lambda_i^n = \dfrac{\delta u_i''^{nT}\,\delta u_i'^{n}}{P^T P - \delta u_i'^{nT}\,\delta u_i'^{n}}$ |
| Second method | $\delta\lambda_i^n = \dfrac{\Delta\lambda_1^n P^T \delta u_i''^{n}}{(K^{n-1T} K^{n-1} - 1)\times P^T \Delta u_1^n}$ |

## 3. NUMERICAL SAMPLES

Based on the proposed Equations (16) and (24), a nonlinear geometric analysis computer program is provided. To be sure, the school program was utilized to find the accurate answers, as well. For years, this nonlinear finite element program has been used in the authors' engineering school, and it has been proved to be free of errors. Several benchmark problems with geometric nonlinear behavior are investigated. With respect to the number of increments and iterations needed to find the structural equilibrium paths; the abilities of the proposed techniques are evaluated. It should be emphasized; the analysis' important properties of each sample are notified in its subsection.

### *3.1 Seven-member truss*

As demonstrated in Fig. 3, the planar truss structure is under concentrated load P. This structure has seven degrees of freedom. The cross-sectional area of the horizontal members is 54.85 $cm^2$ and for the others is 51.56 $cm^2$, correspondingly. The members' modulus of elasticity is 6889.4 $kN/cm^2$. This truss was used to verify higher-order stiffness matrix in the prediction of structural behavior [24]. Furthermore, it was employed for investigating the elastic buckling of members [25]. In this research, the reference load, the arc length of the first loading step, the maximum number of iterations in each increment and the residual error are assumed to be 1 kN, 0.01, 10 and $10^{-4}$, respectively.

The load-deformation curves of node 1 in the vertical direction, and for the node 2 in the horizontal direction are drawn in Fig. 4 and 5, respectively. According to the results, both structural equilibrium paths have the load and displacement limit points. In spite of the fact that these nodes have complex behavioral curves, both proposed methods are able to trace entirely the relevant load-displacement diagram.

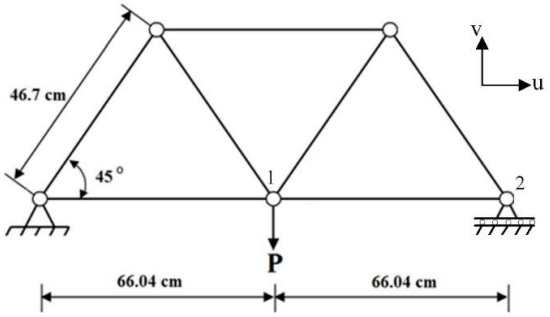


Figure 3. Seven-member truss

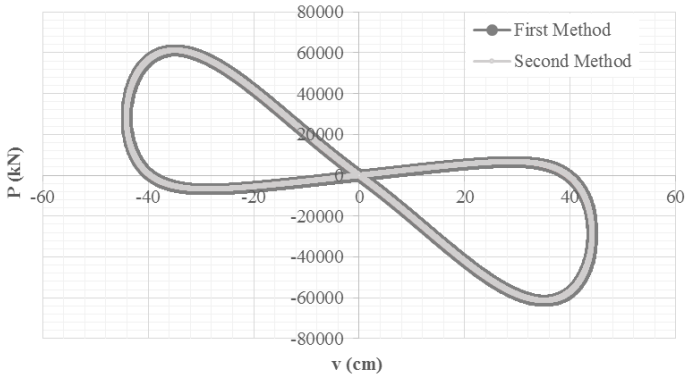


Figure 4. The static curve of seven-member truss of node 1 at vertical direction

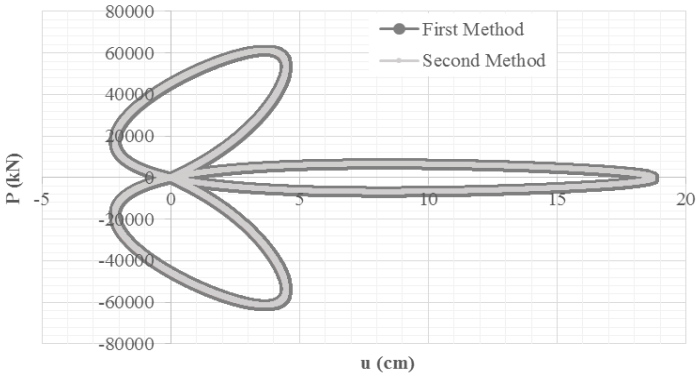


Figure 5. The static curve of seven-member truss of node 2 at horizontal direction

The number of increments and iterations are listed in Table 2. It should be noted, these responses for node 1 are analogous to node 2. According to the obtained results, the first technique can terminate the nonlinear analysis with much fewer increments and iterations than the second solution. In other words, although the second procedure captures all limit points of truss analysis, but it requires more time for analyzing the structure. Consequently, the first proposed method is more powerful in solving this problem.

Table 2: Analysis results of seven-member truss for node 1 or 2

| Constraint | Number of increments | Number of iterations |
|---|---|---|
| First method | 30559 | 30986 |
| Second method | 41741 | 42640 |

*3.2 Two-member truss*

A two-dimensional truss with two degrees of freedom under a concentrated load, is displayed in Fig. 6. Young's modulus of the members is 6889.4 kN/cm$^2$ and their cross-sectional areas are 96.77 cm$^2$. This benchmark was numerically analyzed by Papadrakakis [16]. In another research, this truss was analyzed to check the accuracy of the higher-order stiffness matrix [24]. To solve this two-member truss, the reference load, arc length of the initial loading step, the maximum number of iterations in each increment and the tolerance of the response convergence are considered to be 1 kN, 0.1, 10 and $10^{-4}$, correspondingly.

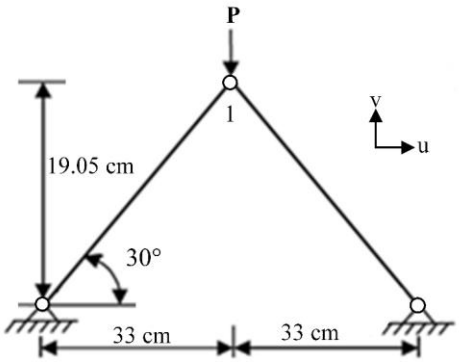


Figure 6. Two-member truss

Fig. 7 indicates the structural equilibrium path of node 1 in the vertical direction which is obtained by the authors' schemes. Evidently, both new strategies can pass through the load limit point. Based on the Fig. 7, the critical load value of this truss is compatible with the one obtained by Torkamani *et al.* [24].

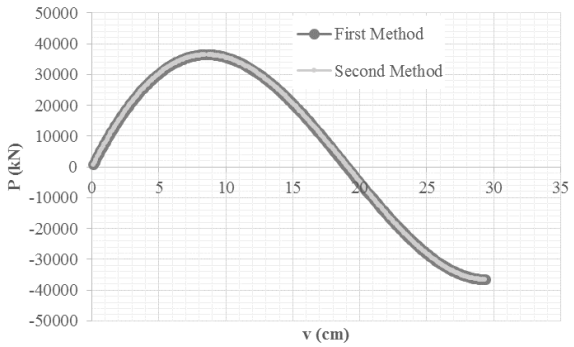


Figure 7. The equilibrium curve of two-member truss's node 1 at vertical direction

In fact, the second recommended procedure is an approximately method because of selecting only the diagonal stiffness matrix arrays for the analysis process. Nevertheless, based on Table 3, this procedure traces the equilibrium curve with fewer numbers of increments and iterations than the first one. By a little difference, analysis of the two-member truss via the second strategy takes the first rank.

Table 3: Analysis results of two-member truss

| Constraint | Number of increments | Number of iterations |
|---|---|---|
| First method | 294 | 600 |
| Second method | 290 | 579 |

*3.3 Five-story frame*

Fig. 8 depicts a planar frame under the horizontal concentrated forces, and the vertical uniform distributed loads. The uniform distributed loads, applied to all beams, have the value of 10 kN/cm. This structure is modeled as a 29-element frame by supposing every beam or column member as one element. It should be added that the dynamic relaxation method was utilized for analyzing this benchmark problem, as well [26].

The elasticity modulus of all members is $2\times10^4$ kN/cm$^2$. Other specifications of structure's beams and columns are registered in Table 4. It should be informed; the equivalent nodal forces and moments of the uniform distributed loads are computed and used for the inputs of the computer program. In this paper, arc length of the first loading step, maximum iterations of each increment and residual error equal to 0.1, 10 and $10^{-4}$, respectively.

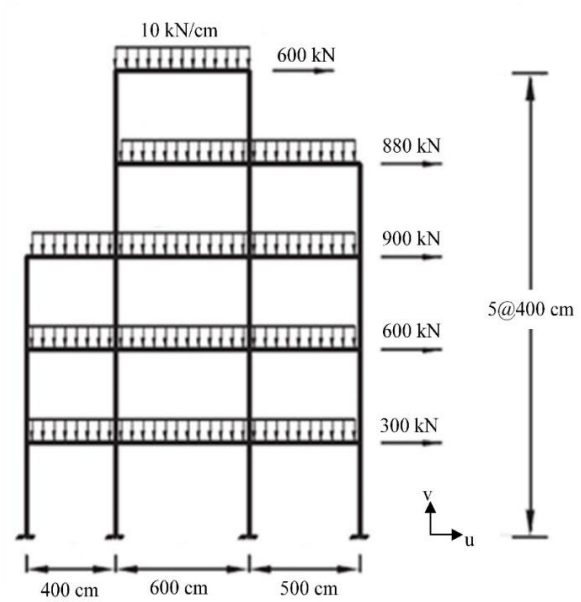


Figure 8. Five-story frame

Table 4: The properties of five-story frame's beams and columns

| Member | Cross-sectional area ($cm^2$) | Moment of inertia ($cm^4$) |
|---|---|---|
| Beam | 66.45 | 21227.8 |
| Column | 94.84 | 40957.17 |

The load-displacement responses of the five-story frame's roof level via novel constraints are depicted in Fig. 9. According to this chart, both algorithms have the ability to find the structural equilibrium path for this frame. It should be added that the resulted curves are fully compatible with the other studies [26].

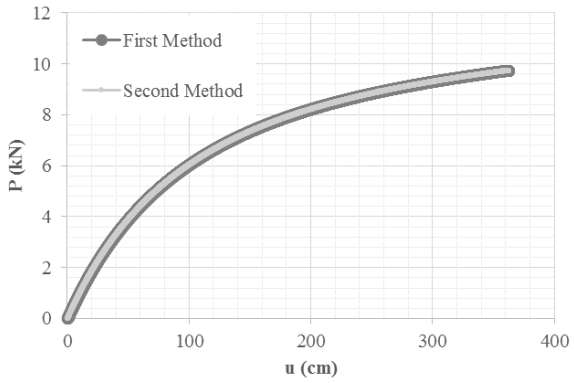


Figure 9. The load-displacement path of five-story frame's roof at horizontal direction

Comparing the findings of nonlinear analysis recorded in Table 5, illustrates that the second method needs 91824 iterations to analyze the structure. However, with the same number of increments, the first method completes the load-deflection curve of the frame with 91893 iterations. Thus, both novel solutions analyze this two-dimensional frame in almost the same time.

Table 5: Analysis results of five-story frame

| Constraint | Number of increments | Number of iterations |
|---|---|---|
| First method | 10000 | 91893 |
| Second method | 10000 | 91824 |

*3.4 Star shaped dome truss*

A three-dimensional truss of Fig. 10 is under the vertical load P = 1 kN in the center. This dome has 13 nodes and 24 members. Young's modulus and cross-sectional area of members equal to $3.03\times10^5$ $N/cm^2$ and 3.17 $cm^2$, correspondingly. This benchmark structure is mostly considered for nonlinear analysis of three-dimensional trusses. For instance, star shaped dome truss was used to investigate the buckling effect on the overall stability of structure [27] and also assessing the ability of an automatic method to reveal the more precise

structural equilibrium path [28]. In addition, Rezaiee-Pajand *et al.* utilized the dynamic relaxation process for tracing the structural equilibrium curve of this truss [29, 30]. In this study, the initial loading step's arc length, maximum iterations of each increment and the residual error are assumed 0.1, 10 and $10^{-4}$, respectively.

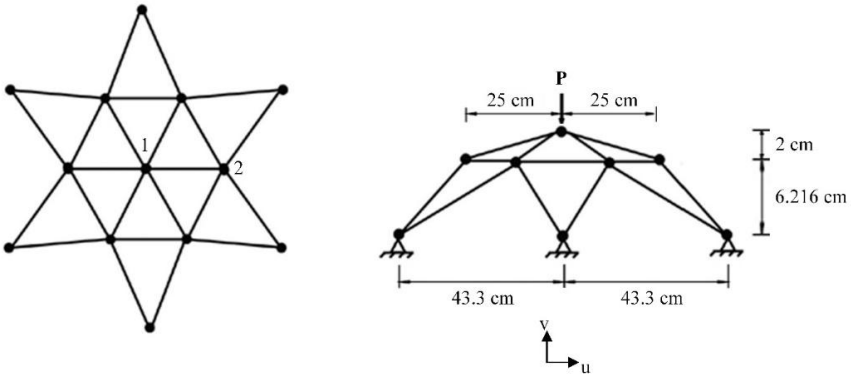


Figure 10. Plan and view of star shaped dome truss

At the first stage, the vertical displacement of node 1 is studied. The obtained load-displacement graph is exposed in Fig. 11. It should be added that the vertical axis of the graph is shown dimensionless. This truss has snap-through behavior at node 1. Based on Fig. 11, the first proposed algorithm can pass limit points and yields the whole equilibrium path. Whereas, the second suggested solver is not able to catch the first limit point, and the related analysis was stopped there.

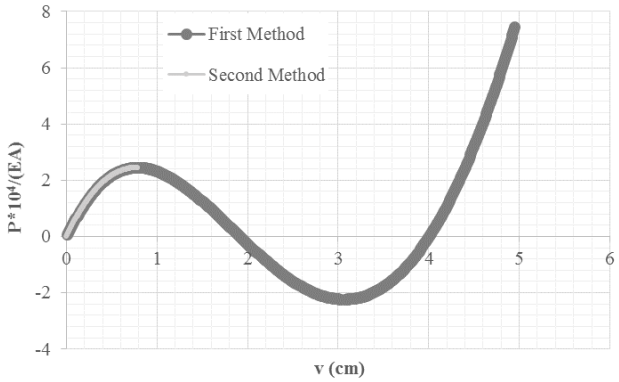


Figure 11. The load-deflection curve of star shaped dome truss of node 1 at vertical direction

The total number of analysis' increments and iterations are inserted in Table 6. The first new technique traverses the curve, which is shown in Fig. 11, with 500 increments and 1006 iterations. The second new procedure is capable of tracing small part of the structural equilibrium path by 160 increments and 350 iterations.

Table 6: Analysis results of star shaped dome truss for node 1 or 2

| Constraint | Number of increments | Number of iterations |
|---|---|---|
| First method | 500 | 1006 |
| Second method | 160 | 350 |

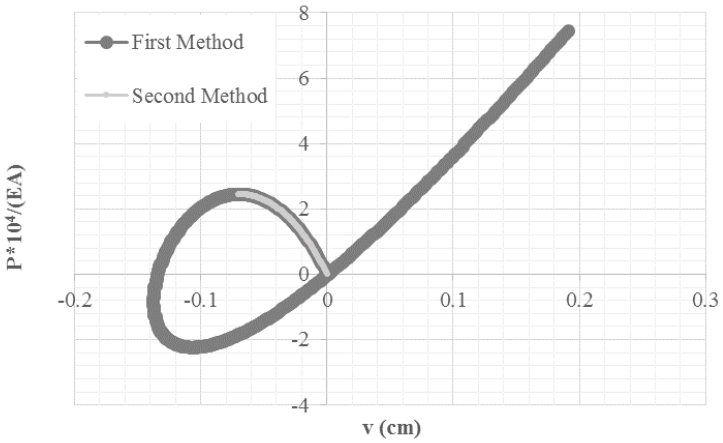


Figure 12. The load-deflection curve of star shaped dome truss of node 2 at vertical direction

In another analysis of this three-dimensional structure, the vertical displacement of the node 2 is checked. The related equilibrium curve has snap-through and snap-back regions. In accordance with Fig. 12 and similar to the results' interpretation of node 1, the first novel procedure crosses every limit points successfully, but the other presented algorithm fails to catch the first limit point. It should be pointed out; the obtained results are compatible with predecessor findings [27].

The significant results of this node are analogous to the ones on Table 6. Eventually, it is concluded that the first strategy, which can accurately trace the structural equilibrium path for the specified nodes, is superior than the second one.

### *3.5 Schwedler's dome truss*

Plan and view of the Schwedler's dome truss are displayed in Fig. 13. This truss has 97 nodes and 264 members. All the peripheral nodes are hinged at the support. All axial stiffness of the members are $6.4\times10^5$ kN. Load P, which is applied on the central node, equals to 1 kN. To find the geometric nonlinear behavior of the three-dimensional trusses; Schwedler's truss was used [31]. Rezaiee-Pajand *et al.* analyzed this benchmark problem to verify orthogonal strategies and also minimum residual length, perimeter and area methods [11]. Moreover, Saffari *et al.* gained the structural equilibrium path of this dome structure by applying the two-point strategy [20]. In this article, inputs of the program for the arc length of initial loading step, maximum number of iterations in each increment and residual error are 0.1, 10 and $10^{-4}$, correspondingly.

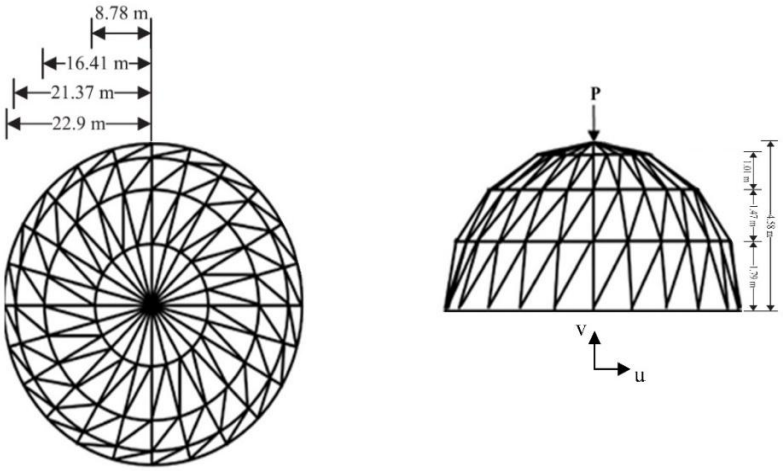


Figure 13. Plan and view of Schwedler's dome truss

To investigate the ability of novel constraints given in Table 1, Schwedler's dome truss is analyzed. The load-displacement curve of the vertical displacement of the highest node is demonstrated in Fig. 14. It can be seen, there are two load limit points in this structural equilibrium curve. The first solver captures the limit points and entirely traverses the relevant equilibrium path. However, the second strategy just represents a small part of the central node's behavior.

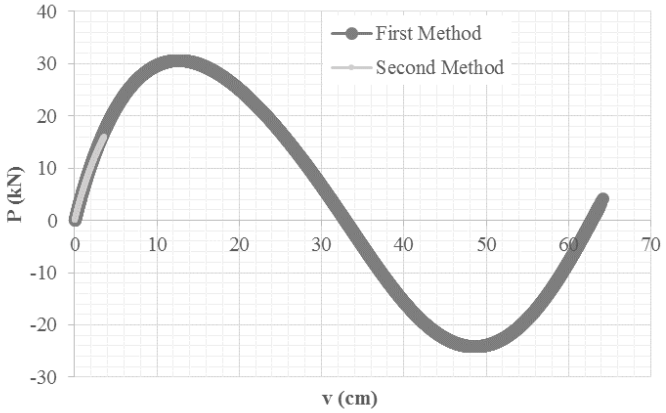


Figure 14. The load-deformation curve of Schwedler's dome truss's crest at vertical direction

In Table 7, two main parameters of analysis are registered. The first solution thoroughly traces the structural load-displacement curve with 5209 increments and 52090 iterations. The second solver incompletely passes the structural equilibrium curve. It is stopped in the 576-th increment and with 5760 iterations. Hence, the first presented solver is successful in the nonlinear analysis of this structure.

Table 7: Analysis results of Schwedler's dome truss

| Constraint | Number of increments | Number of iterations |
|---|---|---|
| First method | 5209 | 52090 |
| Second method | 576 | 5760 |

*3.6. Arc frame*

Fig. 15 displays a two-dimensional structure under an asymmetric loading. This arc structure is designed by authors and is modeled by 33 elements. In addition, this frame has two fixed supports. The elasticity modulus of all members is 6896.4 kN/cm$^2$. Furthermore, the cross-sectional area and the moment of inertia of the members are equal to 309.68 cm$^2$ and 7631.62 cm$^4$, correspondingly. It should be mentioned, the reference load, the arc length of the first loading step, maximum iterations of each increment and the residual error are considered 1 kN, 0.1, 10 and $10^{-4}$, respectively.

The load-displacement responses of the arc frame for node 1 are shown in Fig. 16. According to this diagram, both new schemes can represent the same structural equilibrium path. It should be noted that the obtained curves are compatible with the results of the other algorithms, as well.

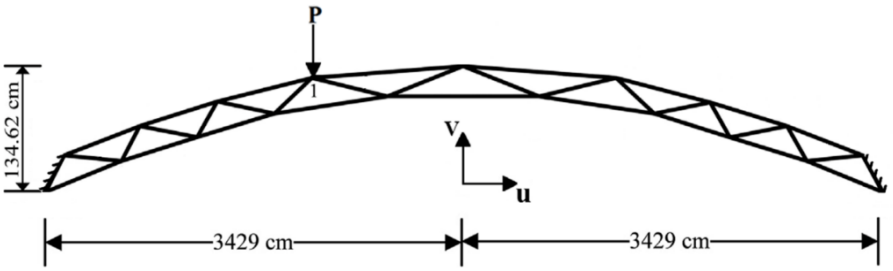


Figure 15. Arc frame

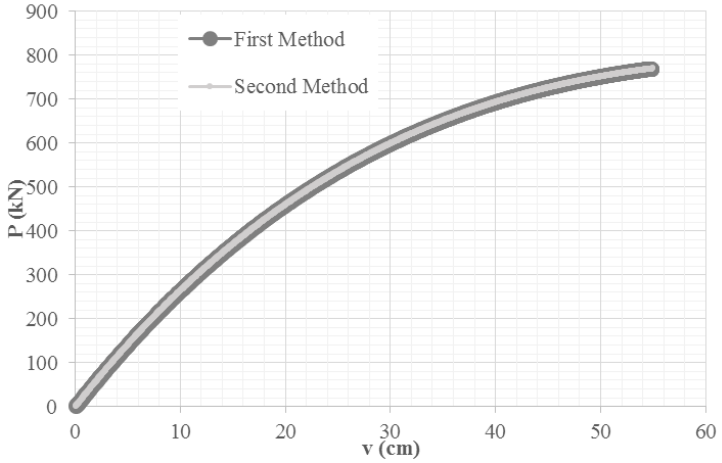


Figure 16. The load-displacement path of arc frame of node 1 at vertical direction

The findings of nonlinear analysis are recorded in Table 8. As illustrated in this table, the second novel strategy analyzes the frame with fewer numbers of increments and iterations than the first suggested technique. In other words, using the second constraint of Table 1, for nonlinear analysis of this structure, is more efficient than another solution.

Table 8: Analysis results of arc frame

| Constraint | Number of increments | Number of iterations |
|---|---|---|
| First method | 1320 | 4350 |
| Second method | 1293 | 3799 |

## 4. CONCLUSION

In the advanced incremental-iterative methods, a load factor is assumed at the beginning of each analysis increment. This part is called the predictor step. By performing the iterative process, the hypothetical obtained point will converge towards the structural equilibrium path. This stage is called the corrector step. In this paper, two objective functions were established. These functions consist of two independent variables, namely, the load factor and the angle between predictor and corrector surfaces. By optimizing these goal functions, two new constraint equalities for the load factor increment were obtained. Since the authors' formulas were general, one more constraint equation was also found that was similar to one of the former nonlinear solvers. By this new way, the previous method was once again mathematically verified. To evaluate the novel schemes, proposed constraints were applied in the geometric nonlinear analysis of several truss and frame structures. The benchmark samples had snap-through or snap-back behaviors. The outcomes of numerical tests illustrated that the first recommended technique could trace structural equilibrium paths in snap-through and snap-back regions and had acceptable compatibility with the previous researches. On the other hand, based on the numerical results, the first suggested technique was more qualified than the other nonlinear solver. It should be emphasized; the second proposed method is rooted in the use of only main diagonal arrays of the structural stiffness matrix in forming the related constraint equation.

## REFERENCES

1. Chen WF, Lui EM. *Stability Design of Steel Frames*, CRC press, 1991.
2. Zienkiewicz OC. Incremental displacement in non-linear analysis, *Int J Numer Meth Eng* 1971; **3**(4): 587-92.
3. Wempner GA. Discrete approximations related to nonlinear theories of solids, *Int J Solids Struct* 1971; **7**(11): 1581-99.
4. Riks E. The application of Newton's method to the problem of elastic stability, *J Appl Mech* 1972; **39**(4): 1060-5.

5. Riks E. An incremental approach to the solution of snapping and buckling problems, *Int J Solids Struct* 1979; **15**(7): 529-51.
6. Ramm E. Strategies for tracing the nonlinear response near limit points, *Nonlinear Finite Elem Anal Struct Mech* 1981; 63-89.
7. Crisfield MA. A fast incremental/iterative solution procedure that handles "snap-through", *Comput Struct* 1981; **13**(1): 55-62.
8. Tsai CT, Palazotto AN. A modified Riks approach to composite shell snapping using a high-order shear deformation theory, *Comput Struct* 1990; **35**(3): 221-6.
9. Bergan PG. Solution algorithms for nonlinear structural problems, *Comput Struct* 1980; **12**(4): 497-509.
10. Chan SL. Geometric and material non-linear analysis of beam-columns and frames using the minimum residual displacement method, *Int J Numer Meth Eng* 1988; **26**(12): 2657-69.
11. Rezaiee-Pajand M, Tatar M, Moghaddasie B. Some geometrical bases for incremental-iterative methods, *Int J Eng, Trans B: Appl*, 2009; **22**(3): 245-56.
12. Yang YB, Shieh MS. Solution method for nonlinear problems with multiple critical points, *AIAA J* 1990; **28**(12): 2110-6.
13. Cardoso EL, Fonseca JSO. The GDC method as an orthogonal arc-length method, *Commun Numer Meth Eng* 2007; **23**(4): 263-71.
14. Allgower EL, Georg K. Homotopy methods for approximating several solutions to nonlinear systems of equations, *Numer Solut Highly Nonlinear Prob* 1979; **72**: 253-270.
15. Saffari H, Fadaee MJ, Tabatabaei R. Nonlinear analysis of space trusses using modified normal flow algorithm, *J Struct Eng* 2008; **134**(6): 998-1005.
16. Papadrakakis M. Inelastic post-buckling analysis of trusses, *J Struct Eng* 1983; **109**(9): 2129-47.
17. Rezaiee-Pajand M, Taghavian-Hakkak M. Nonlinear analysis of truss structures using dynamic relaxation, *Int J Eng, Trans B: Appl*, 2006; **19**(1): 11-22.
18. Rezaiee-Pajand M, Alamatian J. Nonlinear dynamic analysis by dynamic relaxation method, *Struct Eng Mech* 2008; **28**(5): 549-70.
19. Rezaiee-Pajand M, Estiri H. Mixing dynamic relaxation method with load factor and displacement increments. *Comput Struct* 2016; **168**: 78-91.
20. Saffari H, Mansouri I. Non-linear analysis of structures using two-point method, *Int J Non-Linear Mech* 2011; **46**(6): 834-40.
21. Saffari H, Mirzai NM, Mansouri I. An accelerated incremental algorithm to trace the nonlinear equilibrium path of structures, *Latin American J Solids Struct* 2012; **9**(4): 425-42.
22. Rezaiee-Pajand M, Ghalishooyan M, Salehi-Ahmadabad M. Comprehensive evaluation of structural geometrical nonlinear solution techniques Part I: Formulation and characteristics of the methods, *Struct Eng Mech* 2013; **48**(6): 849-78.
23. Batoz JL, Dhatt G. Incremental displacement algorithms for nonlinear problems, *Int J Numer Meth Eng* 1979; **14**(8): 1262-7.
24. Torkamani MAM, Shieh JH. Higher-order stiffness matrices in nonlinear finite element analysis of plane truss structures, *Eng Struct* 2011; **33**(12): 3516-26.

25. Timoshenko SP, Gere JM. *Theory of Elastic Stability*, McGraw-Hill, New York, 1961.
26. Rezaiee-Pajand M, Sarafrazi SR, Rezaiee H. Efficiency of dynamic relaxation methods in nonlinear analysis of truss and frame structures, *Comput Struct* 2012; **112**: 295-310.
27. Tanaka K, Kondoh K, Atluri SN. Instability analysis of space trusses using exact tangent-stiffness matrices, *Finite Elem Anal Des* 1985; **1**(4): 291-311.
28. Ligarò S, Valvo P. A self-adaptive strategy for uniformly accurate tracing of the equilibrium paths of elastic reticulated structures, *Int J Numer Meth Eng* 1999; **46**(6): 783-804.
29. Rezaiee-Pajand M, Sarafrazi SR. Nonlinear dynamic structural analysis using dynamic relaxation with zero damping, *Comput Struct* 2011; **89**(13): 1274-85.
30. Rezaiee-Pajand M, Alamatian J. Automatic DR structural analysis of snap-through and snap-back using optimized load increments, *J Struct Eng* 2010; **137**(1): 109-16.
31. Greco M, Gesualdo FAR, Venturini WS, Coda HB. Nonlinear positional formulation for space truss analysis, *Finite Elem Anal Des* 2006; **42**(12): 1079-86.